M.H. KABIR,[1] M.B. ALAM MIAH,[1] S. ASADUZZAMAN,[1,2] K. AHMED[1]

[1] Department of Information and Communication Technology, Mawlana Bhashani Science and Technology University
(Santosh, Tangail-1902, Bangladesh; e-mail: sayed.swe@diu.edu.bd, samonna25@gmail.com)
[2] Department of Software Engineering, Daffodil International University, Dhaka, Bangladesh
(e-mail: sayed.swe@diu.edu.bd, samonna25@gmail.com)

UDC 539

SLOTTED CORE CIRCULAR PCF IN CHEMICAL SENSING APPLICATIONS

A circular photonic crystal fiber including slotted core (SC-PCF) is proposed for chemical sensing application. The full vectorial finite-element method (FEM) has been applied for a numerical investigation by altering geometrical metrics in the interval of wavelengths from 0.7 to 1.5 μm. An optimized structure is selected by investigating the proposed PCF. The main focus of this research is to find out the hazardous and toxic chemicals. The proposed structure shows a relative sensitivity of 47.08% and a confinement loss of 3.11 × 10^{-5} dB/m at the same time.

Keywords: slotted core, finite-element method, photonic crystal fiber, photonic bandgap fiber.

1. Introduction

Photonic crystal fibers (PCFs) are ones consisting of periodically arrangeed tiny air holes in a cladding, and the core region contains a silicon background of materials with low and high refractive indices [1]. It is a low-loss dielectric medium that runs all over the entire fiber length. With the contribution of PCFs, the modern fiber optic technology has greatly emerged in recent years. PCFs have some unique properties. For that reason, researchers have a high attraction to PCF. It contains cylindrical air holes in the cladding that are periodic. It is a single or multimode fiber. In the core materials, air or silica is present. On the other hand, the cladding materials are silica-air microstructures.

PCFs can be divided into two categories such as photonic bandgap (PBG) fibers [2, 3] and index guiding (IG) fibers [4, 5]. A PBG fiber is a microstructure of periodic elements and a core of low-index materials (hollow core). Light is guided by a photonic bandgap principle. On the other hand, an IG fiber is a solid-core conventional fiber. In an IG fiber, light can be guided through a low-index core by the photonic crystal reflection of a cladding.

PCFs can be used as liquid or chemical sensors [6–8], filters [9], switches [10], gas sensors [11–14], and electro-optical modulators [15] *etc.* The first fabricated PCF was hexagonal [16]. Nowadays, a lot of PCFs such as octagonal [17], decagonal [18], with honeycomb cladding [19], circular [20], and hybrid shaped [21] are designed to achieve better guiding properties.

In the modern advance manufacturing technology, PCFs have a lot of guiding properties such as the high relative sensitivity [22], high nonlinear effect [23], high birefringence [24], and ultra-flattened dispersion [25]. PCFs can be used for the optical communication [26], nonlinear optics [27], high-power technology [28], spectroscopy [29], supercontinuum generation [30], and sensing applications like chemical and gas sensings.

In 2007, Yue *et al.* used elliptical holes and got a high birefringence. In 2011, J. Park *et al.* [31] increased the relative sensitivity for chemical sensing applications with hexagonal arrangement of air holes. They improved the sensitivity to 5.09% from 4.79%; the confinement loss to 1.25 dB/m from 32.4 dB/m as compared to prior PCFs [32]. In 2014, H. Ademgil [33] proposed the performance of liquid sensors and found better sensing properties with low confinement loss for O-PCF as compared with H-PCF.

In this paper, SC-PCFs, where the arrangement of the core is of slotted shape, have been proposed,

and their guiding properties are numerically investigated. Finally, it is found that SC-PCFs increase the relative sensitivity as compared to prior PCFs for chemical sensing applications over a wide range of wavelengths.

2. Geometrical Structure of the proposed SC-PCF

Figure 1 shows the transverse cross-section of the proposed SC-PCF. From Fig. 1, it is clear that the proposed SC-PCF is circular shaped with three rings of holes in the cladding region, where the first, second, and third rings of a hole includes 6, 12, and 18 circular air holes, respectively. The diameters of the first, second, and third rings were the same assumed as d. The distance between the centers of two adjacent air holes is called a pitch. The hole-to-hole distance of two adjacent air holes in the cladding is denoted by Λ_1. The circular area of the core region is defined as D.

The proposed SC-PCF contains three slotted core holes in the core, where the major and minor axes of the holes are assumed as da and db. The pitch between two adjacent holes of the core is denoted by Λ. The core holes are filled with ethanol (with a refractive index of 1.354). The thickness of the perfectly matched layer (PML) of a proposed SC-PCF is set around 10% between the inner and outer parts having a silica background. The refractive index of silica varies according to the Sellmeier equation.

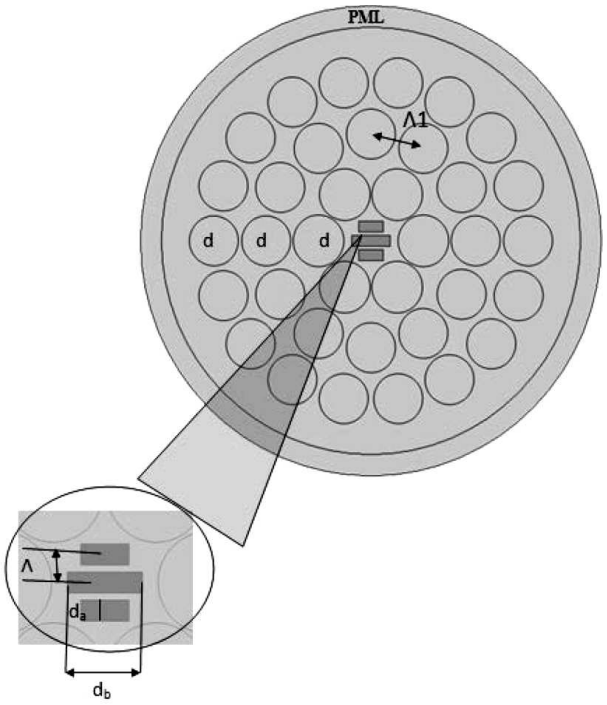

Fig. 1. Transverse cross-section of the proposed SC-PCF

3. Synopsis of Numerical Method

The full vectorial finite-element method (FEM) is applied to the circular perfectly matched layer (PML) to investigate the proposed SC-PCF. The propagation characteristics and optical properties of the leaky modes can be evaluated, by using PML's boundary condition in a wide interval of wavelengths from 0.7 to 1.5 μm. To model the background material, the Sellmeier equation is used. The refractive index of silica varies with the variation of the wavelength according to the equation

$$n(\lambda) = \sqrt{1 + \frac{B_1\lambda^2}{\lambda^2 - C_1} + \frac{B_2\lambda^2}{\lambda^2 - C_2} + \frac{B_3\lambda^2}{\lambda^2 - C_3}}, \qquad (1)$$

where n is the refractive index of silica, λ (μm) is the wavelength, and B_i, (i = 1, 2, 3,) and C_i, (i = 1, 2, 3) are the Sellmeier coefficients. Using the anisotropic PML, the following vectorial equation is derived from Maxwell's equations:

$$\nabla([S]^{-1})\nabla E - K_0^2 n^2 [S]E = 0, \qquad (2)$$

where $K_0 = 2\pi/\lambda$ is the wave number in free space, n is the refractive index of the domain, E is the electric field, $[s]$ is the PML matrix, $[S]^{-1}$ is an inverse matrix of $[s]$, and λ is the operating wavelength. The leaking of light from the core to exterior materials results in the confinement loss L_C, which can be obtained from the imaginary part of n_{eff}, by using the following equation. The confinement loss

$$L_C = \frac{40\pi}{\ln(10)\lambda}\text{Im}(n_{\text{eff}}) \times 10^6 \approx 8.686 K_0 \text{Im}(n_{\text{eff}}) \times 10^6. \qquad (3)$$

The relative sensitivity coefficient measures the interaction between light and the material to be sensed, and it can be calculated through the equation

$$r = \frac{n_r}{n_{\text{eff}}} f, \qquad (4)$$

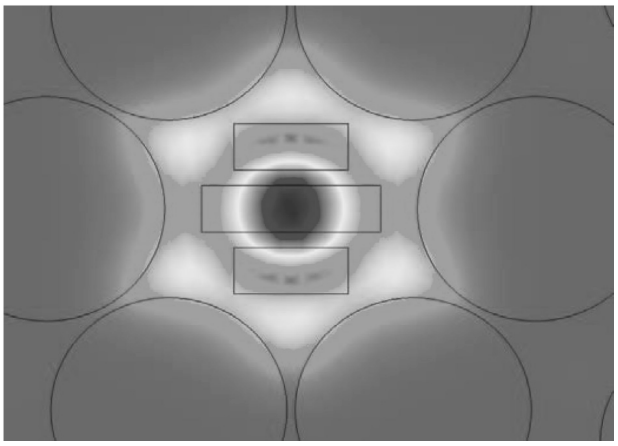

Fig. 2. Power flow distribution in the proposed SC-PCF

where n_r is the refractive index of the sample (ethanol) to be sensed, and n_{eff} is the modal effective index; f is the percentage ratio of a power within the core and the total power, and it is also known as the power distribution function. With the use of Poynting's theorem, it can be expressed as follows:

$$f = \frac{\int_{\text{sample}} \text{Re}(E_x H_y - E_y H_X) d_x d_y}{\int_{\text{total}} \text{Re}(E_x H_y - E_y H_X) d_x d_y}, \qquad (5)$$

where E_x and H_x are the transverse electric and magnetic fields, E_y and H_y are the longitudinal electric and magnetic fields. Using the finite-element method (FEM), the mode field pattern (E_x, H_x, E_y, H_y) and the effective index n_{eff} are calculated.

4. Result and Discussions

The optical properties of the proposed SC-PCF vary according to the geometrical parameters. The guiding properties with regard for the geometrical parameter have been investigated, by using the software COMSOL Multiphysics 5.0. The power flow distributions of x- and y-polarizations for ethanol at the operating wavelength $\lambda = 1.33$ μm are shown in Fig. 2. The figure shows that the interaction of light occurs through the core region, where the analyte is present. The figure also indicates that the mode field is tightly confined at the core region.

Figure 3 illustrates a variation of the slotted core area diameter, which is responsible for changing the guiding properties of the SC-PCF structure. The core area diameter variation means a variation of the size

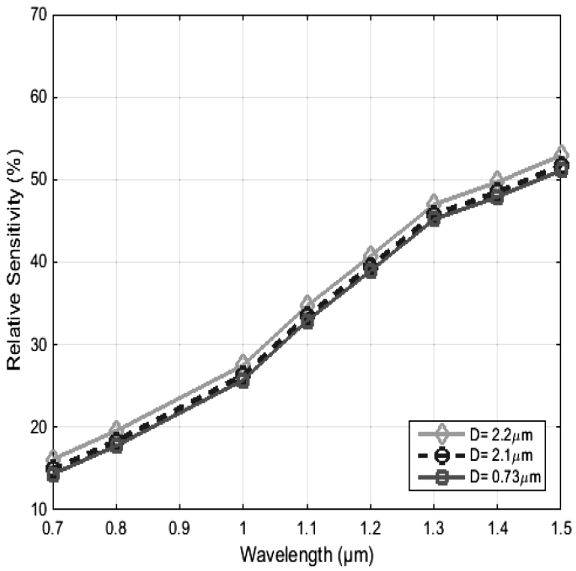

Fig. 3. Relative sensitivity versus the wavelength for $D = 2.20$ μm, $D = 2.10$ μm, $D = 0.73$ μm

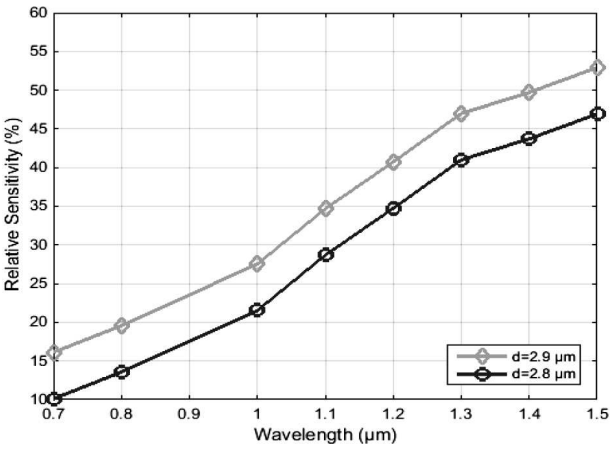

Fig. 4. Relative sensitivity versus the wavelength for different diameters of cladding holes; $d = 2.90$ μm, $d = 2.8$ μm

of slots with respect to the wavelength. The relative sensitivity does not change a lot with a variation of D. The sensitivity increases sharply with the wavelength.

Figure 4 describes the impact of changing the cladding hole diameters. For the bigger diameter for cladding air holes, the sensitivity is relatively high, and it increases gradually with the wavelength. In addition, the proposed PCF shows a higher confinement loss for small diameters of air holes.

Comparison of the simulated results and the structure shape for the proposed PCF and prior PCFs for ethanol at $\lambda = 1.33$ μm

PCF	Sensitivity (%)	Confinement loss	Core Shape	Cladding Shape
Proposed PCF	47.08	3.11×10^{-5}	Slotted	Circular
Prior PCF1	23.05	5.74×10^{-6}	Circular hole	Circular holes in octagonal configuration
Prior PCF2	23.75	2.4×10^{-4}	Elliptic holes	Elliptic holes in hexagonal configuration

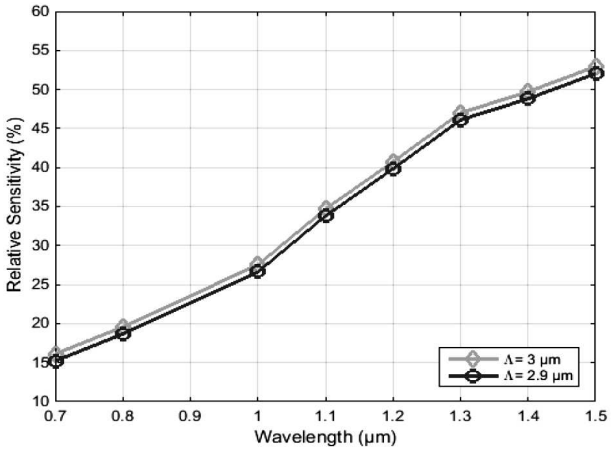

Fig. 5. Relative sensitivity versus the wavelength for different pitch values

Figure 5 shows that a little bit impact on the relative sensitivity occurs for changing the pitch value. The figure clearly shows that the relative sensitivity increases linearly from the 0.7-μmwavelength to the-1 μm one, and then it increases gradually. The comparison between previous and proposed PCFs has been shown in Table. From Table, it it is seen that the proposed PCF shows a higher relative sensitivity and a lower confinement loss at the same time. The fabrication of such type of PCF is challenging. For the fabrication of a crystalline or amorphous structure, the extrusion technique [30] can be used. So, to extrude the slotted-core area of the proposed SC-PCF, this method can be used. Drilling and drawing [31] and the sol-gel method [32] can be used to fabricate the proposed PCF. A structure with experimental demonstration that it can be used as a chemical sensor with core filled with chemicals (Ethanol) was proposed by Zhang *et al.* [32].

5. Conclusion

We have numerically demonstrated that a slotted-core PCF can be used for sensing applications. The proposed model presents the high sensitivity as a chemical sensor. It also shows a lower confinement loss. Due to the advancement of nanotechnology, the proposed PCF can be fabricated. Guiding properties of the SC-PCF has been analyzed to reveal the proposed structure usability. The main goal of this research is to detect low-index chemicals.

1. J.C. Knight. Photonic crystal fibers. *Nature* **424**, 847 (2003).
2. J.C. Knight, J. Broeng, T.A. Birks, P.S.J. Russell. Photonic band gap guidance in optical fiber. *Science* **282**, 1476 (1998).
3. J.M. Fini. Microstructure fibers for optical sensing in gasses and liquids. *Meas. Sci. Technol.* **15**, 1120 (2004).
4. J.C. Knight, T.A. Birks, P.S.J. Russell, D.M. Atkin. All-silica single-mode optical fiber with photonic crystal cladding. *Opt. Lett.* **21**, 1547 (1996).
5. T.A. Birks, J.C. Knight, P.S.J. Russell. Endlessly single-mode photonic crystal fiber. *Opt. Lett.* **22**, 961 (1997).
6. K. Ahmed, M. Morshed. Design and numerical analysis of microstructured-core octagonal photonic crystal fiber for sensing applications. *Sensing and Bio-Sensing Research.* **7**, 1 (2016).
7. K. Ahmed, S. Asaduzzaman, M.F.H. Arif. Numerical analysis of O-OPCF structure for sensing applications with high relative sensitivity. In *2nd International Conference on Electrical Information and Commmunication Technology (EICT), Bangladesh, 2015.*
8. S. Asaduzzaman, K. Ahmed, M.F.H. Arif, M. Morshed. Application of microarray-core based modified photonic crystal fiber in chemical sensing. In *1st International Conference on Electrical and Electronics Engineering, Bangladesh, 2015.*
9. M. Arjmand, R. Talebzadeh. Optical filter based on photonic crystal resonant cavities. *Optoelectronics and Advanced Materials-Rapid Communications* **9** (1-2), 32 (2015).
10. K. Fasihi. High-contrast all-optical controllable switching and routing in nonlinear photonic crystals. *J. of Lightwave Technology* **32** (18), 3126 (2014).
11. M. Morshed, M.F.H. Arif, S. Asaduzzaman, K. Ahmed. Design and characterization of photonic crystal fiber for sensing applications. *Eur. Sci. J.* **11**, 228 (2015).

12. M. Morshed, S. Asaduzzaman, M.F.H. Arif, K. Ahmed. Proposal of simple gas sensor based on micro structure optical fiber. In *2nd International Conference on Electrical Engineering and Information & Communication Technology, Bangladesh, 2015*.
13. M. Morshed, M.I. Hassan, T.K. Roy, M.S. Uddin, S.M.A. Razzak. Microstructure core photonic crystal fiber for gas sensing applications. *Appl. Optics.* **54**, 8637 (2015).
14. M. Morshed, M. I. Hasan, S.M.A. Razzak. Enhancement of the sensitivity of gas sensor based on microstructure optical fiber. *Photonic Sensors* **5** (4), 312 (2015).
15. J.M. Brosi, C. Koos, L.C. Andreani, *et al.* High-speed low-voltage electro-optic modulator with a polymer-infiltrated silicon photonic crystal waveguide. *Optics Express* **16** (6), 4177 (2008).
16. J.C. Knight, T.A. Birks, P.S.J. Russell, D.M. Atkin. All-silica single-mode optical fiber with photonic crystal cladding. *Opt. Lett.* **21** (19), 1547 (1996).
17. H. Ademgil. Highly sensitive octagonal photonic crystal fiber based sensor. *Optik-Intern. J. for Light and Electron Optics* **125**, 6274 (2014).
18. S.A. Razzak, M.A.G. Khan, F. Begum, S. Kaijage. Guiding properties of a decagonal photonic crystal fiber. *J. of Microwaves, Optoelectr., and Electromagn. Appl.* **6** (1), 44 (2007).
19. Y. Hou, F. Fan, Z.-W. Jiang, X.-H. Wang, S.-J. Chang. Highly birefringent polymer terahertz fiber with honeycomb cladding. *Optik-Intern. J. for Light and Electron Optics* **124** (17), 3095 (2013).
20. S. Asaduzzaman, M.F.H. Arif, K. Ahmed, P. Dhar. Highly sensitive simple structure circular photonic crystal fiber-based chemical sensor. In: *IEEE Intern. WIE Conference on Electrical and Computer Engineering (WIECON-ECE) 2015*, pp. 151–154.
21. M. Morshed, M.F.H. Arif, S. Asaduzzaman, K. Ahmed. Design and characterization of photonic crystal fiber for sensing applications. *Eur. Sci. J.* **11** (12), 228 (2015).
22. M. Morshed, M.I. Hasan, S.A. Razzak. Enhancement of the sensitivity of gas sensor based on microstructured optical fiber. *Photonic Sensors* **5**, 312 (2015).
23. F. Begum, Y. Namihira, S.A. Razzak, S. Kaijage, N.H. Hai, T. Kinjo, K. Miyagi, N. Zou. Design and analysis of novel highly nonlinear photonic crystal fibers with ultra-flattened chromatic dispersion. *Opt. Commun.* **282**, 1416 (2009).
24. M.S. Habib, M.S. Habib, S.A. Razzak, M.A. Hossain. Proposal for highly birefringent broadband dispersion compensating octagonal photonic crystal fiber. *Opt. Fiber Technol.* **19**, 461 (2013).
25. M.S. Habib, M.S. Habib, M.I. Hasan, S.A. Razzak. A single mode ultra flat high negative residual dispersion compensating photonic crystal fiber. *Opt. Fiber Technol.* **20**, 328 (2014).
26. F. Zolla, G. Renversez, A. Nicolet, B. Kuhlmey, S. Guenneau, D. Felbacq, A. Argyros, S. Leon-Saval. *Foundations of Photonic Crystal Fibers* (World Scientific, 2005).
27. H. Ebendorff-Heidepriem, P. Petropoulos, S. Asimakis, V. Finazzi, R. Moore, K. Frampton, F. Koizumi, D. Richardson, T. Monro. Bismuth glass holey fibers with high nonlinearity. *Opt. Express* **12** (21), 5082 (2004).
28. C. Lecaplain, B. Ortaç, G. Machinet, J. Boullet, M. Baumgartl, T. Schreiber, E. Cormier, A. Hideur. High-energy femtosecond photonic crystal fiber laser. *Opt. Lett.* **35** (19), 3156 (2010).
29. R. Holzwarth, T. Udem, T.W. Hänsch, J.C. Knight, W.J. Wadsworth, P.S.J. Russell. Optical frequency synthesizer for precision spectroscopy. *Phys. Rev. Lett.* **85** (11), 2264 (2000).
30. J.M. Dudley, G. Genty, S. Coen. Supercontinuum generation in photonic crystal fiber. *Rev. Mod. Phys.* **78** (4), 1135 (2006).
31. J. Park, S. Lee, S. Kim, K. Oh. Enhancement of chemical sensing capability in a photonic crystal fiber with a hollow high index ring defect at the center. *Optics Express* **19**, 1921 (2011).
32. J. M. Fini. Microstructure fibres for optical sensing in gases and liquids. *Meas. Sci. Technol.* **15** (6), 1120 (2004).
33. H. Ademgil. Highly sensitive octagonal photonic crystal fiber based sensor. *Optik-Intern. J. for Light and Electron Optics* **125**, 6274 (2014).

Received 08.03.17

М.Х. Кабір, М.Б. Алам Міаха, С. Асадуззаман, К. Ахмед

ВОЛОКНО КРУГОВОГО ПЕРЕРІЗУ З ФОТОННИМ КРИСТАЛОМ І ЩІЛИНОВИДНОЮ СТРУКТУРОЮ ДЛЯ ВИЯВЛЕННЯ ХІМІЧНИХ РЕЧОВИН

Р е з ю м е

Запропоновано волокно кругового перетину з фотонним кристалом і щілиновидною структурою для виявлення хімічних речовин. Використано загальний векторний метод кінцевих елементів для чисельних розрахунків з мінливою геометрією в інтервалі довжин хвиль 0,7–1,5 мкм. Як результат, вибрано оптимальну структуру. Основний напрямок цієї роботи полягає у виявленні шкідливих токсичних речовин. Запропонована структура має відносну чутливість 47,08 % і, в той же час, загасання конфайнмента $3{,}11 \cdot 10^{-5}$ дБ/м.